# Evidence for age-related vulnerability in dopamine-glutamate projections to the lateral entorhinal cortex

**Authors**: Jacquelyn N. Tomaio[1], Sixtine Fleury[1,2], Alexandra Bilder[1], Jordan Nacimba[1], Abhilash Lakshman[1,3], Yoon Seok Kim[4], Lief Ericsson Fenno[4,6], Charu Ramakrishnan[5], Karl Deisseroth[7,8,9], Susana Mingote[1,*]

**Affiliations**:
[1]Advanced Science Research Center at the Graduate Center, CUNY, New York, NY, USA.

[2]Department of Psychological and Brain Sciences, Dartmouth College, Hanover, NH, USA.

[3]Gill Institute for Neuroscience and Department of Biology, Indiana University, Bloomington, IN, USA.

[4]Department of Neurology and Neurological Sciences, Stanford University, Stanford, CA 94305, USA.

[5]Stanford University, Stanford, CA, USA.

[6]Department of Psychiatry & Behavioral Sciences, The University of Texas at Austin, Dell Medical School, Austin, Texas, USA.

[7]Department of Bioengineering, Stanford University, Stanford, CA 94305, USA.

[8]Department of Psychiatry and Behavioral Sciences, Stanford University, Stanford, CA, USA.

[9]Howard Hughes Medical Institute, Stanford, CA 94305, USA.

*Correspondence should be addressed to Dr. Susana Mingote: 85 Saint Nicholas Terrace, 4th Floor Neuroscience Initiative, New York, NY 10031 USA (S.M.)

Email Address: smingote@gc.cuny.edu (S.M.)

# Abstract

The lateral entorhinal cortex (LEC) is selectively vulnerable to age-related decline and is essential for novelty detection and episodic memory. While DAergic (DAergic) input is known to modulate LEC function, how aging impacts this circuitry remains unclear. Here, we used two viral labeling strategies to investigate projections from the ventral tegmental area (VTA) to the LEC. First, we employed an INTRSECT dual-recombinase approach in TH-Flp::VGLUT2-Cre mice to selectively label dopamine-only (DA-only) and dopamine-glutamate co-releasing (DA-GLU) neurons. Next, we used a DAT-Cre-driven ChR2-YFP strategy to broadly label all DA axons. We found that both DA-only and DA-GLU populations innervate the LEC. With age, we observed a selective reduction in tyrosine hydroxylase (TH) signal within DA axons in the LEC, despite preserved axonal structure as revealed by YFP labeling. VGLUT2 signal within DA-GLU terminals appeared less affected. In the VTA, TH+ neuron density declined with age, with distinct spatial patterns along the anterior-posterior axis. These findings reveal an age-related vulnerability of DAergic projections to the LEC and suggest a circuit-level mechanism may contribute to memory impairments in aging.



# Key words

Aging, dopamine-glutamate co-transmission, lateral entorhinal cortex, ventral tegmental area, memory, INTRSECT

# Introduction

Aging can be accompanied by a progressive decline in cognitive abilities, among which episodic memory impairment is especially prominent (Gallagher and Rapp, 1997; Wilson et al., 2006; Alexander et al., 2012). Episodic memory enables the recall of specific events in their contextual framework, and its degradation contributes to many of the challenges faced by older individuals, including an attenuated response to novelty, difficulty discriminating new from familiar experiences and vulnerability to false memories and interference (Norman and Schacter, 1997; Wilson et al., 2006; Reagh et al., 2016). These changes occur in the absence of neurodegeneration and are thought to reflect subtle, circuit-level alterations in temporal lobe regions critical for memory (Rapp and Gallagher, 1996, 1996; Yassa et al., 2010; Reagh and Yassa, 2017; Tran et al., 2019).

Among medial temporal lobe structures, the lateral entorhinal cortex (LEC) emerges as one of the earliest and most selectively vulnerable regions in both normal aging and preclinical Alzheimer's disease (Khan et al., 2014; Reagh et al., 2018; Tran et al., 2022). Human imaging studies show that reduced LEC activation correlates with impairments in object recognition and discrimination in older adults (Reagh et al, 2018). The LEC is critical involved in novelty detection and item-context integration (Deshmukh and Knierim, 2011; Hunsaker et al., 2013; Tsao et al., 2013; Vandrey et al., 2020; Persson et al., 2022), yet the circuit-level mechanisms underlying its dysfunction and how they drive age-related deficits in recognition and associative memory remain poorly understood.

Dopamine (DA) neurons in the ventral tegmental area (VTA) signal the novelty and salience of incoming stimuli (Schultz, 1998; Bromberg-Martin et al., 2010; Kutlu et al., 2021) and modulate recognition memory (Osorio-Gómez et al., 2022; Fleury et al., 2024). Novelty-induced DA signaling modulates memory by regulating synaptic plasticity in the hippocampus (Huang and Kandel, 1995; Lisman and Otmakhova, 2001; Li et al., 2003; Tsetsenis et al., 2023). However, anatomical studies in mice reveal that DAergic projections from the VTA to the hippocampus are sparse, and that most novelty-induced dopamine release originates from locus coeruleus noradrenergic neurons. (Smith and Greene, 2012; Kempadoo et al., 2016; Takeuchi et al., 2016). In contrast, the LEC receives dense DAergic innervation from the VTA (Swanson, 1982; Mingote et al., 2015), positioning it as a key substrate for novelty-driven DAergic modulation of memory. Indeed, recent work has shown that DAergic signaling in the LEC facilitates associative memory formation by encoding novelty cues. (Lee et al., 2021). It is well established that DAergic signaling is altered in the aged brain (Bäckman et al., 2006), including within temporal lobe regions (Morcom et al., 2010), and that such alterations affect novelty processing in aging (Bunzeck et al., 2007; Chowdhury et al., 2012). How these changes impact the VTA–LEC pathway has not been directly examined.

Over the past two decades, it has become clear that VTA neurons consist of molecularly and functionally distinct subpopulations capable of co-releasing additional neurotransmitters (Tritsch et al., 2012; Eskenazi et al., 2021). Among these, dopamine–glutamate (DA–GLU) neurons represent a unique subpopulation. (Stuber et al., 2010; Root et al., 2016; Mingote et al., 2019; McGovern et al., 2024). These DA-GLU neurons exhibit strong responses to salient stimuli and are contribute to behavioral flexibility and the actions of drugs of abuse (Mingote et al., 2017, 2019; Buck et al., 2021; Eskenazi et al., 2021; McGovern et al., 2024; Warlow et al., 2024). DA–GLU neurons rely on the vesicular glutamate transporter VGLUT2 for glutamate loading and release (Stuber et al., 2010; Wang et al., 2017) and make strong glutamatergic connections to the LEC neurons (Mingote et al., 2015). Co-transmission from VTA dopamine neurons is

increasingly recognized as sensitive to aging, with reduced TH and VGLUT2 mRNA expression observed in aged mice (Buck et al., 2025).

We hypothesized that age-related impairments in novelty recognition and associative memory may stem from disruptions in VTA DAergic input to the LEC, particularly within the DA-GLU subpopulation. To test this, we employed the INTRSECT (Fenno et al., 2020) viral labeling approach in TH-FLP::VGLUT2-Cre mice to selectively trace DA-only and DA-GLU neurons in the VTA and quantify their terminal projections to the LEC across lifespans. We combined anatomical mapping with immunohistochemical quantification to assess how aging alters this neuromodulatory circuit. Our findings reveal a selective vulnerability of LEC-projecting DA-GLU neurons, offering new insight into the circuit-specific basis of memory decline in aging.

# Results

***Labeling DA-GLU and DA-only Neurons in the VTA Using an Intersectional Strategy***

To distinguish DAergic neurons that co-release glutamate (DA-GLU) from those that release only dopamine (DA-only), we used an intersectional viral approach (INTRSECT 2.0; (Fenno et al., 2020) in double transgenic mice (TH-flp/+::VGLUT2-cre/+; **Fig. 1A**, *top*). These mice express *flp* recombinase under the tyrosine hydroxylase (TH) promoter, marking DA neurons, and *cre* recombinase under the VGLUT2 promoter, marking glutamatergic neurons.

To broadly target the VTA, we injected a mixture of two INTRSECT viruses into both the middle VTA and the lateral VTA/substantia nigra (**Fig. 1A**, *middle*). The virus AAV8-Con/Fon-EYFP labels neurons that co-express *flp* and *cre*, thereby identifying DA-GLU neurons via EYFP expression. In contrast, AAV8-Coff/Fon-mCherry expresses mCherry in neurons that express *flp* but not *cre*, labeling DA-only neurons (**Fig. 1A**, *bottom; adapted from Fenno et al., 2020*).

We next assessed how accurately the viruses labeled the subpopulations of DA neurons. To determine glutamatergic identity and specificity, we combined VGLUT2 *in situ* hybridization with EYFP and mCherry immunohistochemistry (**Fig. 1B**). Confocal photomicrographs (**Fig. S1A**, *left*) and volume-rendered images (**Fig. S1A**, *right*) of fluorescence-labeled neurons revealed that 93% ± 1.6% of EYFP+ neurons contained VGLUT2 puncta, confirming successful targeting of DA-GLU neurons. mCherry+ neurons had almost no VGLUT2 signal, consistent with their DA-only identity, although 10% ± 1.4% of mCherry+ neurons showed a single VGLUT2 punctum (**Fig. 1C and Fig. S1B**).

To evaluate targeting specificity for DAergic neurons, we quantified co-localization with TH immunostaining. We found that 91% ± 2.9% of mCherry+ neurons and 78% ± 4.1% of EYFP+ neurons were TH+ (**Fig. 1D,E**). The minority of EYFP+ neurons lacking TH immunoreactivity may be part of a previously described subset of VTA neurons expresses TH mRNA but lack detectable TH protein (Yamaguchi et al., 2015). These neurons could be glutamatergic-only (GLU-only) neurons with ectopic EYFP expression, as most EYFP+ neurons also expressed VGLUT2.

Despite a small degree of ectopic EYFP expression in GLU-only neurons, these results demonstrate that the INTRSECT viral strategy is highly effective and selective for labeling DA-GLU neurons with EYFP and DA-only neurons with mCherry, providing a robust tool to distinguish these functionally distinct populations in the VTA and evaluate the effects of aging.

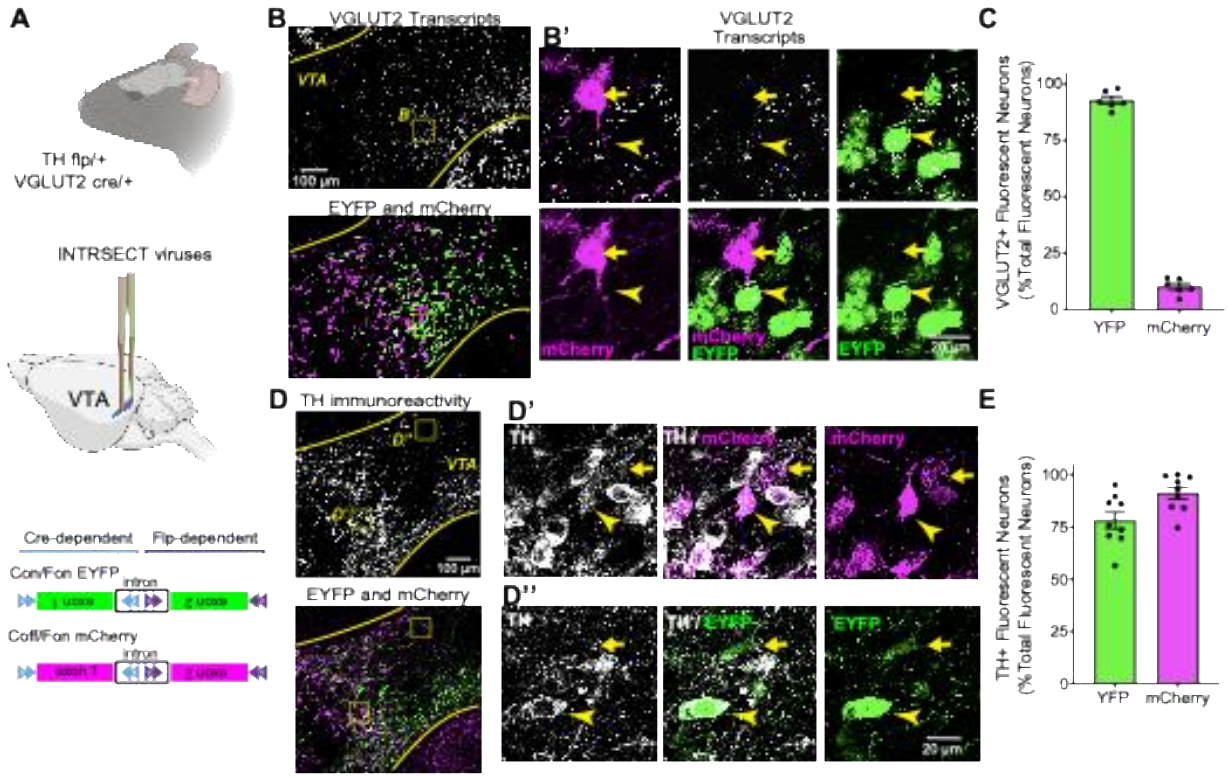


**Figure 1 - Intersectional labeling distinguishes DA–GLU and DA-only neurons in the VTA using INTRSECT viruses.** (**A**) Experimental schematic for double transgenic TH-flp::VGLUT2-cre mice and INTRSECT constructs. Con/Fon drives EYFP in neurons that express both flp and cre (DA–GLU, shown in green) *Figure adapted from Fenno et al. 2020*. Coff/Fon drives mCherry in neurons that express flp but not cre (DA-only, shown in magenta). (**B**) VTA images combining VGLUT2 mRNA *in situ* (top) with EYFP and mCherry immunostaining (bottom); Insert B′ shows EYFP+ somata containing VGLUT2 transcripts and mCherry+ somata containing minimal VGLUT2 signal. (**C**) Quantification of fluorescent neuron subtypes co-expressing VGLUT2 mRNA and EYP (green) or VGLUT2 mRNA and mCherry (magenta), expressed as the percentage of total fluorescently labeled neurons. EYFP+ neurons show high VGLUT2 co-expression. (**D**) Confocal images of VTA sections showing fluorescent labeling of TH+ (top), EYFP+ and mCherry+ neurons (bottom); Insert D' shows TH immunoreactivity and merged overlays with mCherry; Insert D'' shows TH immunoreactivity and merged overlays with EYFP. (**E**) Quantification of fluorescent neuron subtypes co-expressing TH protein and EYP (green) or TH protein and mCherry (magenta), expressed as the percentage of total fluorescently labeled neurons. Bar graphs display mean percentages with SEM.

### *Distribution of Subpopulations of Dopamine Neurons in the VTA and LEC in Young Mice*

DA neuron subpopulations show distinct prevalence and spatial distribution patterns within the ventral tegmental area (VTA) (**Fig. 2A–C**). We found that 36% of all fluorescently labeled cells in the VTA were EYFP+, and when limiting the analysis to TH+ neurons, 33% of transfected TH+ VTA neurons were EYFP+ DA-GLU neurons. This proportion is consistent with prior reports in mice, which estimate DA-GLU neurons to comprise 20–30% of the VTA DA population using intersectional genetic labeling or multiplex *in-situ* hybridization (Yamaguchi et al., 2015; Poulin et al., 2018; Mingote et al., 2019; Eskenazi et al., 2021; Conrad et al., 2024). We observed no differences between males and females; therefore, the data were combined (**Fig. S2A–C**).

DA-GLU and DA-only neurons also differ in their anatomical distribution. YFP+ DA-GLU neurons are enriched in the interfascicular nucleus (IF), rostral linear nucleus (RLi), and the paranigral part (PBP) of the VTA (**Fig. 2A**; Conrad et al., 2024). Along the anterior-posterior axis (-3.2 to -3.7 mm from bregma), DA-GLU neurons were predominantly located in the posterior VTA, whereas mCherry+ DA-only neurons were more concentrated in the anterior VTA (**Fig. 2D**, *right*). A two-

way repeated measures ANOVA (2 (cell type) by 6 (distances from bregma, as the within-subject factor)) revealed significant effects of cell type ($F(1, 8) = 40.36$, $p < .0001$, $\eta p^2 = .31$), distance from bregma ($F(5, 40) = 6.85$, $p < .0001$, $\eta p^2 = .28$), and their interaction ($F(5, 40) = 5.58$, $p < .001$, $\eta p^2 = .24$), all in the large effect size range. Post-hoc Bonferroni comparisons indicated that mCherry+ neuron density was significantly greater than EYFP+ at –3.4 mm ($p = .011$), –3.3 mm ($p = .004$), and –3.2 mm ($p = .001$), but not at more posterior levels.

When examining DAergic projections to the lateral entorhinal cortex (LEC), a region known to be especially vulnerable to aging, we found that 93% of labeled axons were EYFP+, indicating that nearly all DAergic input to the LEC originates from DA-GLU neurons (**Fig. 2E–G**). This was a surprising and novel finding, given the DA-GLU neurons constitute only a minority population within the VTA. Importantly, it builds on our earlier functional connectome work showing robust glutamatergic input from DA neurons to LEC neurons using patch-clamp recordings (Mingote et al., 2015) and together these results validate that DA-GLU neurons play a dominant role in modulating LEC function.

In summary, intersectional strategies reveal that DA-GLU neurons make up roughly one-third of VTA DA neurons, are concentrated in the posterior medial VTA, and provide the majority of DAergic innervation to the LEC.

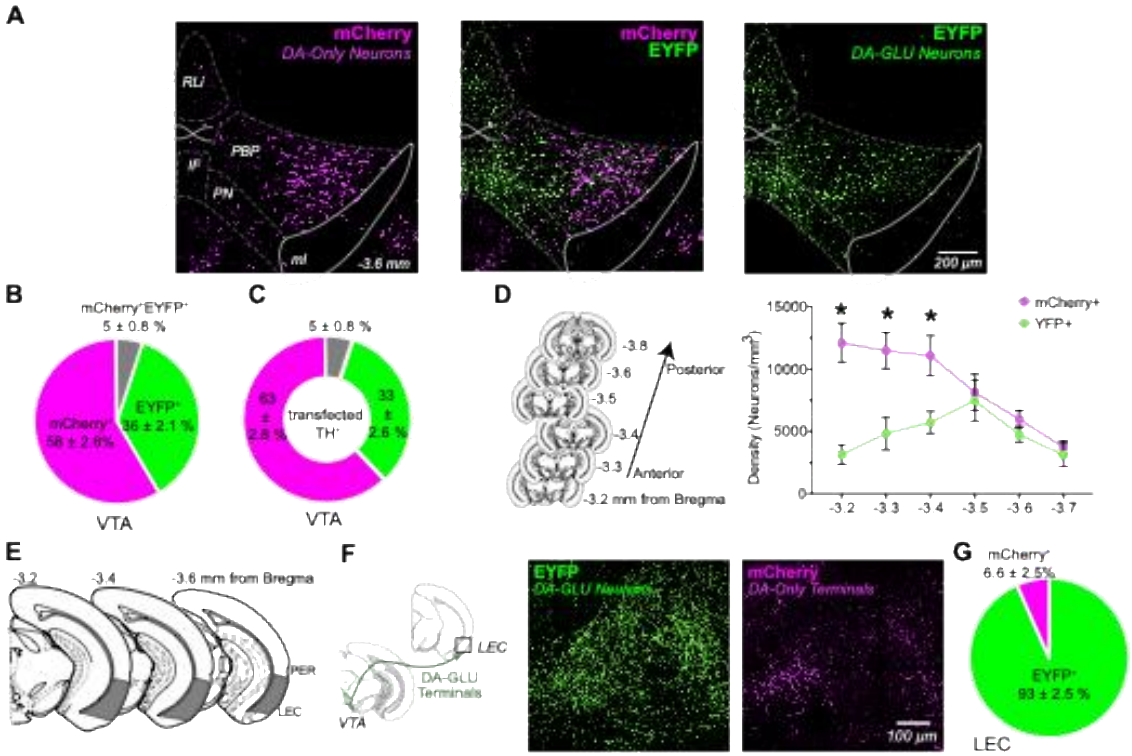


**Figure 2. DA–GLU and DA-only neurons exhibit distinct spatial organization in the VTA and differentially innervate the lateral entorhinal cortex in young mice.** (**A**) Distribution of INTRSECT labeled VTA neurons expressing EYFP (DA–GLU, green), mCherry (DA-only, magenta), and merge (middle). (**B**) Proportion of EYFP+ (green), mCherry+ (magenta), and co-localized EYFP+/ mCherry+ (gray) neurons in the VTA. (**C**) Proportion of EYFP+/TH+ (green), mCherry+/TH+ (magenta), and EYFP+/ mCherry+/TH+ (gray) neurons in the VTA. (**D**) Schematic of coronal brain sections used for quantification (left); Line plot showing the density (neurons/mm³) of mCherry+ and EYFP+ neurons across the anterior–posterior VTA axis. two-way repeated measures ANOVA; *significant post hoc comparisons, p<0.05. (**E**) Schematic of coronal brain sections from −3.2 mm to −3.6 mm relative to bregma highlighting the lateral entorhinal cortex (LEC) as region of interest and perirhinal cortex (PER). (**F**) Diagram showing the projection from VTA DA–GLU neurons to the LEC (left); Representative image of DA–GLU axons (EYFP+, green) and DA-only axons (mCherry+, magenta) in the LEC. (**G**) Proportion of fluorescent axons in the LEC that are EYFP+ (green) versus mCherry+ (magenta). Graphs show as mean ± SEM.

***Effects of Aging on the Density of DA Neuron Subpopulations within the VTA***

The age-related decline of the DAergic system is heterogeneous, affecting some forebrain-projecting DAergic VTA pathways but sparing others (Bäckman et al., 2006; Karalija et al., 2022; Nordin et al., 2022; Johansson et al., 2023). Because subpopulations of VTA dopamine neurons innervate distinct brain regions (Eskenazi et al., 2021), we investigated whether aging differentially impacts these specific subpopulations.

We labeled DA-GLU and DA-only neurons using INTRSECT viral strategies in mice of different ages: 3 months (young, n=9), 14 months (middle, n=7), and 24 months (aged/old, n=5) (**Fig. 3A**). Double transgenic mice (TH-flp/+::VGLUT2-cre/+) were injected with a combination of Con/Fon-EYFP and Coff/Fon-mCherry viruses one month before reaching the target age group (young: 2 months, $n$ = 9; middle-aged: 13 months; aged: 23 months), allowing sufficient time for viral expression before perfusion. A one-month period was allowed for viral expression before the mice were perfused. Age did not affect the transfection rate, which we quantified as the percentage of TH+ neurons in the VTA that co-expressed the transgenes (mCherry and YFP combined) relative to the total number of TH+ VTA neurons, for all ages the average percentage of transfected cells was between 72 to 77% (**Fig. 3B**). The aging process also did not alter the specificity of the INTRSECT viruses in targeting DA-GLU versus DA-only neurons (**Fig. S3 A,B**). However, we observed that the overall density of TH+ neurons decreased by ~40% in both middle-aged and aged mice (**Fig. 3C**). One-way ANOVA revealed an age effect: $F(2, 18) = 7.91$, $p = .0034$, with large effect size ($\eta p^2 = .47$). Post-hoc Dunnett's comparisons indicated that density was significantly lower in 14 months ($p = .011$) and 24 months ($p = .004$), relative to 3 months aged mice. To assess whether this age-related decline differentially affected dopamine neuron subpopulations, we separately quantified DA-GLU and DA-only neurons (**Fig. 3D**). DA-only neurons showed a decreasing trend that did not reach statistical significance ($F(2, 18) = 1.95$, $p = .171$, $\eta p^2 = .17$, moderate effect size), whereas the density of DA-GLU neurons was significantly reduced with age ($F(2, 18) = 5.81$, $p = .011$, $\eta p^2 = .39$, large effect size). The density of DA-GLU neurons was significantly lower than in young mice at 14 and 24 months (Post-hoc Dunnett's comparisons, 14 months ($p = .044$) and 24 months ($p = .011$).

We evaluated how density changes along the anterior–posterior axis by comparing 3- and 24-month-aged mice (**Fig. 3E**). For the mCherry+ DA-only subpopulation, a two-way repeated measures ANOVA with Age (between-subjects) and Distance from bregma (–3.2 to –3.7 mm, within-subjects) revealed a robust main effect of Distance ($F(5, 60) = 8.04$, $p < 0.001$, $\eta p^2 = .455$), but no significant main effect of Age ($F(1, 12) = 3.87$, $p = 0.073$, $\eta p^2 = .078$) and no Age × Distance interaction,($F(5, 60) = 0.78$, $p = 0.571$, $\eta p^2 = .061$). In contrast, for the EYFP+ DA-GLU subpopulation, the ANOVA revealed significant main effects of both Distance ($F(5, 60) = 2.81$, $p = 0.024$, $\eta p^2 = .25$) and Age ($F(1, 12) = 8.29$, $p = 0.0138$, $\eta p^2 = .11$), while the Age × Distance interaction was not significant ($F(5, 60) = 1.32$, $p = 0.268$, $\eta p^2 = .10$). These results indicate that although density varies along the anterior–posterior axis for both subpopulations, the Age effect is specific to DA-GLU neurons, reinforcing that the reduction in the density of TH+ neurons at 24 months is primarily driven by loss of TH+ DA-GLU neurons rather than TH+ DA-only neurons.

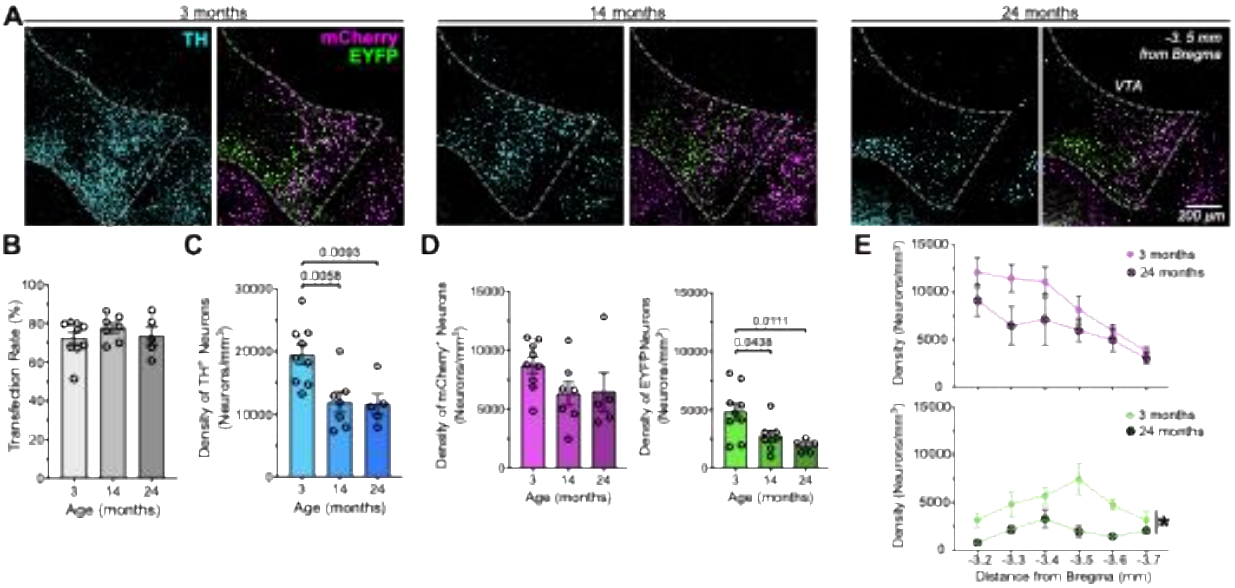


**Figure 3 - The effects of aging on the density of dopamine neuron subpopulations within the ventral tegmental area.** (**A**) Representative unilateral coronal sections through the ventral tegmental area (VTA) at approximately −3.5 mm from bregma in 3- (left), 14- (middle), and 24-month-old (right) mice, showing fluorescent labeling of TH+ (blue), EYFP+ (green), and mCherry+ (magenta) neurons. (**B**) Bar graph showing the transfection rate, calculated as the percentage of TH+ neurons that co-expressed both EYFP and mCherry immunofluorescence, relative to the total number of TH+ VTA neurons, across age groups. (**C**) Bar graph showing TH+ neuron density (neurons/mm³) across age groups (one-way ANOVA with Dunnett's post hoc, *p* values above brackets). (**D**) Bar graph showing mCherry+ (left) and EYFP+ (right) neuron density across age groups (one-way ANOVA, Dunnett's post hoc, *p* values above brackets). (**E**) Line graphs showing the density of mCherry+ (top) and EYFP+ (bottom) neurons across six anterior–posterior VTA distances (−3.2 to −3.7 mm from bregma) in 3- and 24-month-old mice (two-way repeated measures ANOVA, *main effect of age). Error bars shown as mean ± SEM; Statistics detailed in the text and Methods.

### *Effects of Aging on the Density of DAergic Projections to LEC*

Since DA-GLU neurons provide the predominant DAergic input to the LEC, we next asked whether their age-related decline was accompanied by a corresponding reduction in INTRSECT-labeled axons within this region. To quantify terminal density, we performed 3D reconstructions of INTRSECT-labeled axons using volume-rendering software and measured their volume relative to the total volume of the LEC (**Fig. 4A**). We observed a marked reduction in the density of EYFP-labeled DA-GLU axons, in both middle-aged and aged mice (**Fig. 4B**). A Kruskal–Wallis test revealed a significant main effect of age ($H(2) = 9.26$, $p = 0.0097$), with a large effect size ($\eta^2H = 0.56$). Post-hoc Dunn's tests confirmed significant reductions in both 14-month ($p = 0.0258$) and 24-month ($p = 0.0141$) groups compared to 3-month controls. We also assessed whether the smaller population of mCherry+ axons in the LEC was affected by age and found that expression was significantly reduced at 14 months but not at 24 months (Kruskal–Wallis: $H(2) = 9.80$, $p = 0.0074$; Dunn's tests: 14 months, $p = 0.004$; 24 months, $p = 0.070$) (**Fig. 4C**). Overall, YFP labeling showed substantial losses, averaging ~75% in middle-aged mice and approaching complete loss in some aged animals (**Fig. 4A**). Of relevance to this study, although DA-GLU neuron density in the VTA declined by only ~40% at 14 months, this was accompanied by nearly a 75% reduction in INTRSECT-labeled axons in the LEC. This disproportionate decline indicates that the LEC is especially vulnerable to early DA-GLU dysfunction.

We further investigated why INTRSECT labeling of DA-GLU neurons and their axons in the LEC declines with age. A recent study reported that TH and VGLUT2 RNA expression in the VTA decreases in aged mice without evidence of cell loss (Buck et al., 2025). We therefore

hypothesized that reduced expression of TH or VGLUT2 may underlie the diminished INTRSECT labeling, since this viral strategy depends on the activity of both promoters. To test this, we used an alternative viral strategy in which YFP is expressed under the DAT promoter, independent of TH or VGLUT2 expression status. An AAV-FLEX-ChR2-YFP virus was injected into the VTA of DAT-Ires-Cre mice at 2 or 23 months of age to generate young (3-month-old, $n$ = 10) and aged (24-month-old, $n$ = 11) cohorts. With this approach, YFP+ DAergic axons in the LEC were clearly observed in both groups (**Fig. 4D**), and quantification of terminal volume revealed no age-related differences (**Fig. 4E**). A Mann–Whitney U test confirmed the absence of a significant age effect ($U = 68.5$, $p = 0.36$). The small effect size ($r = 0.21$) further indicates that any difference between groups is minimal. Thus, terminal density in the LEC is largely preserved at 24 months. Taken together, these results argue against cell loss or terminal degeneration and instead suggest that the apparent reduction in INTRSECT labeling reflects decreased TH or VGLUT2 expression with age.

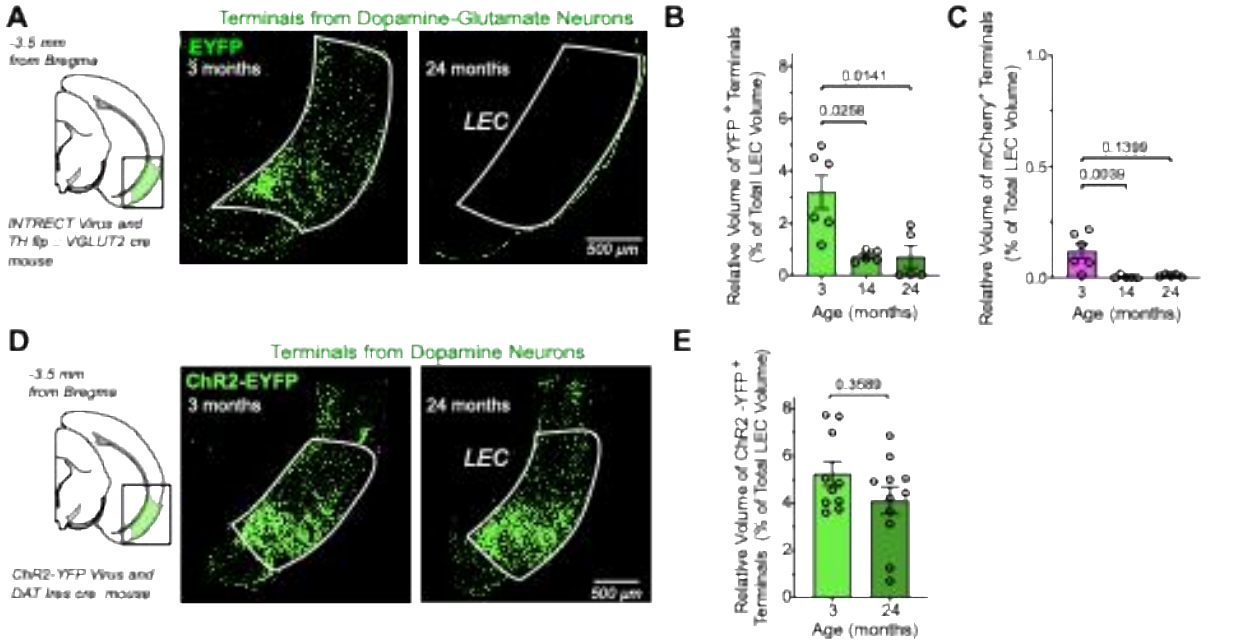


**Figure 4 – Distinct viral labeling strategies show an age-related reduction in LEC-projecting terminals from VTA dopamine-glutamate (DA-GLU) terminals.** (**A**) Schematic of demi-coronal brain section −3.5 mm relative to bregma highlighting the lateral entorhinal cortex (LEC) as region of interest; Representative images showing EYFP-labeled terminals from DA-GLU neurons in the LEC of 3- (left), and 24-month-old (right) TH-FLP::VGLUT2-Cre mice injected with the Cre-On/Flp-On INTRSECT virus. (**B**) Relative volume of EYFP+ terminals in the LEC, expressed as a percentage of total LEC volume. Aged mouse groups showed a significant reduction in EYFP+ terminal volume compared to young mice (unpaired t-test; $p$-values shown on the graph). (**C**) Relative volume of mCherry+ terminals in the LEC, expressed as a percentage of total LEC volume. Aged mouse groups showed a significant reduction in mCherry+ terminal volume compared to young mice (unpaired t-test; $p$-values shown on the graph). (**D**) Schematic of demi-coronal brain section −3.5 mm relative to bregma highlighting the LEC as region of interest; Representative images showing ChR2-EYFP-labeled terminals from DAergic neurons in the LEC of 3- (left), and 24-month-old (right) DAT-Ires-Cre mice injected with the ChR2-EYFP virus. (**E**) Relative volume of ChR2-YFP+ terminals in the LEC, expressed as a percentage of total LEC volume. No significant difference was observed between groups ($p$-value shown on graph). Data are shown as mean ± SEM. Each dot represents one mouse.

### *Decreased Dopamine Synthesis and Glutamate Vesicular Loading with Aging*

We investigated whether YFP-labeled DAergic axons in the DAT-Ires-Cre mouse expressed the proteins TH and VGLUT2. To quantify TH expression, we performed volume rendering and generated surfaces of both TH and YFP immunoreactivity (**Fig. 5A**). TH clusters overlapping by

more than 65% with YFP labeling were considered to be inside YFP+ axons, and the volume of TH inside axons was calculated relative to the total volume of YFP+ axons in the LEC. We quantified the superficial and deep layers of the LEC separately, as these layers are functionally distinct (Canto et al., 2008; Witter et al., 2017; Wang et al., 2023) and YFP+ axons were denser in the superficial layer (**Fig. S4A**). TH expression within YFP+ axons was significantly reduced with age in both layers (**Fig. 5A, B**; superficial layer: $t(17) = 5.51$, $p = 3.8 \times 10^{-5}$, Cohen's $d = 2.53$; deep layer: $t(17) = 4.42$, $p = 3.8 \times 10^{-4}$, Cohen's $d = 2.03$), with both declines representing very large effect sizes. In contrast, total TH volume in the LEC, irrespective of overlap with YFP+ axons, showed no age-related decrease (**Fig. S4B, C**). Since noradrenergic neurons densely innervate the LEC and also express TH (Fallon et al., 1978; Ito and Schuman, 2012; Hernández-Frausto and Vivar, 2024), they may contribute to this apparent preservation of total TH with aging. To test this possibility, we directly compared TH volume inside and outside YFP+ axons. In young mice, TH volume was similar inside and outside, whereas in aged mice TH volume inside axons markedly decreased while TH outside axons increased (**Fig. 5C**). A two-way ANOVA with Age and TH Location as between-factors revealed a significant interaction ($F(1,40) = 22.04$, $p < 0.0001$), a main effect of TH location ($F(1,40) = 12.63$, $p = 0.0010$), and no main effect of age ($F(1,40) = 0.68$, $p = 0.41$). Pairwise comparisons using Fisher's LSD test, restricted to four planned comparisons, showed that in young mice TH inside versus outside YFP+ axons was not significantly different (mean diff. = 6,503, $p = 0.19$), whereas in aged mice TH volume was significantly lower inside than outside axons (mean diff. = –23,221, $p < 0.0001$). Across ages, TH inside axons was significantly reduced in aged relative to young mice (mean diff. = 17,480, $p = 0.0004$), and TH outside was significantly higher in aged than in young mice (mean diff. = –12,244, $p = 0.0093$). These results were confirmed using the more conservative Tukey's HSD test, which showed no difference between inside and outside in young mice ($p = 0.44$; $d = 0.73$, moderate effect), but a robust reduction inside versus outside in aged mice ($p < 0.001$; $d = –2.08$, very large effect), a strong age-related reduction inside YFP+ axons ($p = 0.002$; $d = 2.32$, very large effect), and a modest but significant age-related increase outside axons ($p = 0.044$; $d = –0.98$, large effect).

We then assessed whether VGLUT2 expression is also reduced within YFP-labeled axons. VGLUT2 immunolabeling appeared as densely clustered puncta in the LEC, reflecting expression in both DAergic axons and other glutamatergic inputs, with the latter providing the majority of VGLUT2. The overall volume of VGLUT2 puncta in the LEC did not change with aging (**Fig. S4D, E**). To quantify VGLUT2 inside YFP+ axons, we acquired images with a confocal microscope equipped with Airyscan super-resolution detection (Wu and Hammer, 2021). Compared to conventional confocal microscopy, Airyscan employs a detector array with pixel reassignment and deconvolution, improving lateral resolution to ~120 nm and enhancing signal-to-noise, thereby allowing a more reliable visualization of densely packed puncta. VGLUT2 puncta overlapping by more than 65% with YFP labeling were considered inside YFP+ axons (**Fig. 5D**). Using this conservative criterion, we found that in young mice, only ~0.2 % of total VGLUT2 expression in the LEC was localized inside DAergic axons, confirming that the vast majority of VGLUT2 arises from non-DAergic inputs. As with TH, we analyzed superficial and deep layers separately, calculating the volume of VGLUT2 puncta as a percentage of total YFP+ axonal volume. In the superficial layer, VGLUT2 volume was significantly reduced in aged mice (Mann–Whitney $U = 48.0$, $p = 0.024$), with large effect sizes ($r = 0.60$). In contrast, in the deep layer the difference between ages did not reach significance (Mann–Whitney $U = 39.0$, $p = 0.221$), although effect sizes suggested a modest shift ($r = 0.33$).

In conclusion, TH expression was robustly reduced within DAergic axons of the LEC across both superficial and deep layers, whereas TH expression outside YFP+ axons did not decline with age and even showed a modest increase. Given the dense noradrenergic innervation of the LEC, these results suggest that the age-related loss of TH is selective to DAergic inputs and may

reduce dopamine availability without altering norepinephrine tone. In parallel, VGLUT2 expression declined with aging in a layer-specific manner, reaching significance only in the superficial LEC. Together, these findings indicate that DA-GLU neurons projecting to the LEC undergo marked age-related deterioration, with a substantial loss of dopamine synthesis capacity and a more moderate, regionally restricted decline in glutamate vesicular loading.

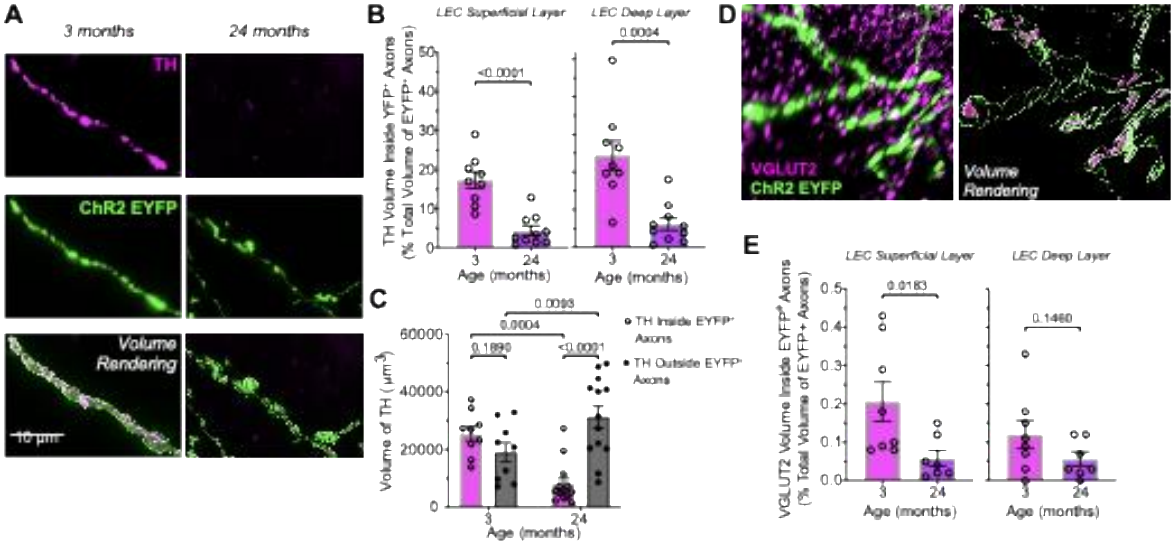


**Figure 5 – Age-related reduction of TH and VGLUT2 content in LEC-projecting DAergic terminals.** (**A**) Representative high-magnification images of axons in the lateral entorhinal cortex (LEC) of 3- (left) and 24-month-old (right) DAT-Ires-Cre mice injected with a ChR2-EYFP. Each column shows TH immunoreactivity (top, magenta), ChR2-EYFP signal (middle, green), and volume rendering (bottom) of merged signals from the same field of view. (**B**) Quantification of TH signal volume within EYFP+ axons, expressed as a percentage of total EYFP+ axon volume, in superficial (left) and deep (right) layers of the LEC. Aged mice exhibited a significant reduction in TH content in both superficial and deep layers (*p*-values shown on graph). (**C**) Absolute volume of TH signal (µm³) within (open circles) and outside (closed circles) EYFP+ axons. (**D**) Representative high-resolution image of VGLUT2 puncta (magenta) colocalized with EYFP-labeled axons (green) in the LEC; raw fluorescence image (left); 3D volume rendering of the same region (right). (**E**) Quantification of VGLUT2 signal volume within EYFP+ axons, expressed as a percentage of total EYFP+ axon volume, in superficial (left) and deep (right) LEC. Aged mice showed a significant reduction in VGLUT2 content in the superficial layer ($p = 0.0183$), with no significant difference in the deep layer ($p = 0.1460$). Scale bars, 10 µm.

# Discussion

The present study identifies a previously unrecognized, age-related decline in TH and VGLUT2 expression within a subpopulation of DA-GLU neurons projecting to the LEC, uncovering their selective vulnerability to aging.

Using intersectional viral strategies, we selectively labeled DA-GLU and DA-only neurons based on the presence or absence of glutamatergic and DAergic marker expression (VGLUT2 and TH, respectively) (Fenno et al., 2020; McGovern et al., 2024; Warlow et al., 2024). These INTRSECT fluorescent reporters, injected at different ages, faithfully reflected endogenous TH and VGLUT2 expression and captured their age-related decline, providing a robust tool to monitor molecular changes within distinct DAergic subpopulations. INTRSECT-induced EYFP labeling of DA-GLU neurons in the VTA and their axons in the LEC was markedly reduced in middle-aged and aged mice. A ~40% decline in VTA DA-GLU neuron density at middle-aged mice was accompanied by an almost 75% reduction in labeled axons in the LEC, indicating that this DAergic projection is

395 particularly vulnerable to early functional decline. Despite the pronounced loss of INTRSECT-
396 driven signal, there was no evidence of axonal degeneration, as DAergic axons remained
397 detectable in aged mice using an alternative DAT promoter-driven viral strategy. Thus, the
398 reduced INTRSECT labeling reflects decreased TH and VGLUT2 expression rather than
399 structural degeneration. While early studies report DAergic neuron loss with aging by measuring
400 pigmented neurons in the substantia nigra (Ma et al., 1999), more recent work using Nissl and
401 DAPI staining in human and mice (Di Lorenzo Alho et al., 2016; Buck et al., 2025) found that
402 although TH expression declines there is no evidence of overt neurodegeneration in the VTA.
403 Consistent with this, our data reveal no major age-related loss of DAergic axons in the LEC, but
404 rather reduced dopamine synthesis and glutamate vesicular loading. This stands in contrast to
405 Alzheimer's disease patients and transgenic mouse models, which report DAergic
406 neurodegeneration in the VTA (Nobili et al., 2017; Serra et al., 2018), particularly within its middle
407 portion where DA-GLU neurons are concentrated. Thus, the molecular alterations we identify in
408 DA-GLU neurons during normal aging may represent an early stage of vulnerability that precedes
409 the neurodegenerative phenotypes observed in Alzheimer's disease.

410 The decline in TH expression within DAergic axons in the LEC was substantial, with some mice
411 exhibiting reductions of up to 80%. This stands in sharp contrast to the absence of an age-related
412 decline in TH expression outside the labeled DAergic axons, presumably noradrenergic neurons.
413 Noradrenergic neurons originating from the locus coeruleus are themselves vulnerable to aging,
414 showing some noradrenergic terminals loss (for review, Leal and Yassa, 2015). We observed a
415 significant increase in TH signal outside the labeled DAergic terminals in aged mice, which may
416 reflect a compensatory mechanism in response to terminal loss, although further studies are
417 needed to test this possibility. Importantly, DAergic axons diverged from these other sources of
418 TH by showing a unique, age-dependent decrease in synthesis, underscoring the cell type- and
419 pathway-specific nature of aging effects within LEC circuitry. A recent study reported reduced TH
420 mRNA levels in the VTA of aged mice without corresponding decreases in TH protein within the
421 nucleus accumbens core or striatum (Buck et al., 2025). Together with our finding of reduced TH
422 expression in the LEC, this suggests that the VTA neurons exhibiting age-related decreases in
423 TH mRNA may be those projecting to the LEC, highlighting the selective vulnerability of this
424 pathway during normal aging. An additional insight from our study is that in brain regions receiving
425 both DAergic and noradrenergic innervation, overall TH levels may be poor indicators of
426 underlying cellular changes, as opposing alterations in different populations can offset one
427 another, as observed here. TH is the rate-limiting enzyme in dopamine synthesis, and reductions
428 in its expression have been shown to decrease dopamine release (Sulzer et al., 2016). Because
429 TH expression is not completely abolished, our data suggest that dopamine release likely persists
430 but may be compromised in a frequency-dependent manner, with the greatest deficits emerging
431 during high-frequency firing when rapid synthesis is required to sustain release. Dopamine
432 neurons typically exhibit pacemaker-like firing at ~4 Hz but transiently increase their activity in
433 bursts of 20–100 Hz to signal salient events in the environment, such as rewards or novel stimuli
434 (Schultz, 1998; Bromberg-Martin et al., 2010; Farassat et al., 2019). Recordings from DA-GLU
435 neurons have shown that these neurons encode the salience of a stimulus independently of its
436 valence, whether positive and rewarding or negative and aversive (McGovern et al., 2024).
437 Therefore, our findings suggest that this phasic mode of salience signaling may be particularly
438 vulnerable to the age-related reduction in TH expression.

439 We also observed a reduction in VGLUT2 expression within DAergic axons in the LEC, which
440 became evident only when the superficial and deep layers were analyzed separately. Two key
441 points emerge from these findings. First, the age-related deficit was restricted to the superficial
442 layers (layers II–III), which represent the principal input layers to the hippocampus. DAergic–
443 glutamatergic signaling in this region could therefore play an important role in filtering which
444 cortical inputs to the LEC influence hippocampal activity. We previously showed that DA-GLU

neurons form strong excitatory connections onto LEC neurons (Mingote et al., 2015), driving robust depolarization and potentially enhancing their responsiveness to sensory inputs. Thus, age-related reductions in VGLUT2 expression may weaken this filtering or gating function, diminishing the ability of the aged brain to regulate information flow to the hippocampus.

Second, the age-related reduction in glutamate vesicular loading was less pronounced than the decline observed in TH expression, suggesting a potential imbalance in dopamine–glutamate co-transmission. Such an imbalance could promote neurotransmitter switching, in which glutamate is released in the absence of dopamine. Similar switching has been reported in DA-GLU neurons of the hypothalamus in response to alterations in the light–dark cycle (Meng et al., 2018). Studies using CRISPR-mediated deletion of either TH or VGLUT2 in DA-GLU neurons have shown that loss of one protein does not affect the expression of the other. That work suggests that DA-GLU neurons projecting to the nucleus accumbens use dopamine signaling to encode aversive events, whereas glutamate transmission predominates during rewarding events. Whether DA-GLU neurons projecting to the LEC follow a similar logic remains unknown; however, if these neurons shift to a glutamate-only phenotype with age, their functional contribution to behavior could be profoundly altered.

The LEC has been a major focus of research since it was first identified as one of the earliest regions in the memory network to exhibit reduced activity with aging (Khan et al., 2014)and subsequent dysfunction in Alzheimer's disease (Small and Swanson, 2018). A hallmark behavioral phenotype associated with LEC dysfunction during aging is impaired pattern separation, in which older individuals and aged rodents show a bias toward perceiving novel events as familiar (Burke et al., 2010; Reagh et al., 2018). Studies in young mice have demonstrated that DAergic signaling in the LEC responds selectively to novelty and facilitates the formation of associative memories (Lee et al., 2021). Thus, a reduction in dopamine release with age could diminish novelty-related signaling in the LEC, leading to a bias toward familiarity. Consistent with this idea, recent studies have shown that dopamine signaling in the LEC is disrupted in a mouse model of Alzheimer's disease and that optogenetic stimulation of these neurons restores associative memory encoding in App-KI mice (Nakagawa et al., 2024). Our findings demonstrate that DA-GLU neurons deteriorate with age, exhibiting deficits in both dopamine synthesis and glutamate vesicular loading. These impairments may trigger a cascade of molecular changes that render the LEC particularly susceptible to age-related dysfunction and contribute to memory decline. In post-mortem tissue from individuals with Parkinson's disease, there is evidence that melanized dopamine neurons in the substantia nigra lose TH expression before undergoing neurodegeneration (Hirsch et al., 1988). Thus, age-related DAergic deficits in the LEC may heighten its vulnerability to Alzheimer's disease, a neurodegenerative disorder for which aging remains the principal risk factor.

# Methods

**Experimental Animals.** All procedures were conducted in accordance with National Institutes of Health *Guide for the Care and Use of Laboratory Animals* and approved by the Institutional Animal Care and Use Committee of the City University of New York (CUNY) Advanced Science Research Center (ASRC). Mice were housed under standard barrier conditions with a 12-hour light/dark cycle and ad libitum access to food and water. Male and female mice were used for all experiments. Two transgenic lines were utilized: (1) TH-Flp;VGLUT2-Cre mice for INTRSECT viral experiments and (2) DAT-IRES-Cre mice for ChR2-YFP labeling. Animals were aged to 2-3 months (young), 13-14 months (middle), or 23-24 months (old).

493 ***Stereotactic Surgery***
494 **INTRSECT Viral Strategy.** To selectively label DA-GLU and DA-only VTA neurons, TH-
495 Flp;VGLUT2-Cre mice were injected with a mixture of AAV8-EF1a-Con/Fon-EYFP-WPRE (labels
496 DA-GLU neurons) and AAV8-EF1a -Coff/Fon-mCherry-WPRE (labels DA-only neurons), following
497 the INTRSECT 2.0 strategy (Fenno et al., 2020). The viruses were kindly donated by Dr.
498 Deisseroth's lab. Injections were performed at 2, 13, or 23 months of age to allow one month of
499 viral expression prior to tissue collection at 3, 14, or 24 months (n = 9, 7, and 5, respectively).
500 Mice were anesthetized with isoflurane (3% induction, 2% maintenance), and 1 µL of viral solution
501 ($1.5 \times 10^{12}$ vg/mL) was pressure-injected into the unilateral VTA and SNc. Stereotaxic coordinates
502 (from bregma) were adjusted by bodyweight: AP –3.0 to –3.4 mm, ML ±0.5 mm, DV –4.1 to –4.5
503 mm. The pipette remained in place for 5 minutes to minimize backflow.
504
505 **ChR2-YFP Strategy.** To label DAergic axons independent of TH or VGLUT2 promoter activity,
506 DAT-IRES-Cre mice were injected bilaterally in the VTA with AAV5-EF1a-DIO-ChR2(H134R)-
507 EYFP (UNC Lot # AV4313-2B; $1.5 \times 10^{12}$ vg/mL) at either 2 months (n = 10) or 23 months (n =
508 11). Coordinates and procedure matched the INTRSECT protocol above.
509
510 ***Immunohistochemistry***
511 **INTRSECT-Labeled Brains.** Immunohistochemistry (IHC) was performed as previously
512 described (Mingote et al., 2017). Mice were anesthetized (ketamine/xylazine) and perfused with
513 PBS followed by 4% paraformaldehyde (PFA). Brains were post-fixed and cut into 50 µm coronal
514 sections. Sections were blocked in 10% NGS with 0.1% Triton X-100 and incubated with primary
515 antibodies:
516 - anti-mCherry (rat, 1:5000; Invitrogen, Cat# M11217)
517 - anti-GFP (chicken, 1:5000; Invitrogen, Cat# A10262)
518 - anti-VGLUT2 (rabbit, 1:250–1:5000; Synaptic Systems, Cat# 135403)
519 Secondary antibodies included Alexa Fluor 488, 568, and 647 conjugates. Imaging was performed
520 using a Leica DM6 B epifluorescence microscope or Zeiss LSM 880 confocal with Airyscan Fast.
521
522 **ChR2-YFP Labeled Brains.** Sections were processed similarly but blocked with 10% NGS and
523 0.5% Triton X-100 in PGBA. Primary antibodies:
524 - anti-TH (chicken, 1:5000; Aves Labs, Cat# TYH)
525 - anti-GFP (rabbit, 1:5000; Abcam, Cat# ab6556)
526 Secondary antibodies were Alexa Fluor 568 and 647 conjugates. Lipofuscin autofluorescence
527 was quenched using cupric sulfate in ammonium acetate (50 mM, pH 5.0) following Schnell et al.,
528 1999. Images were acquired with Leica DM6 B.
529
530 ***In Situ* Hybridization (RNAscope).** *In situ* hybridization was used to detect mRNA transcripts as
531 previously described (Fleury et al., 2024), and combined with IHC following a protocol developed
532 by the manufacturer (ACDBio). RNAscope was performed on 50 µm sections to detect VGLUT2
533 mRNA, combined with immunostaining for EYFP and mCherry. Sections were subjected to heat
534 and protease digestion per manufacturer protocol. Positive control probes were used to validate
535 mRNA detection.
536
537 **Image Acquisition and Quantification.** 3D volume reconstructions and surface renderings were
538 performed using Imaris Bitplane. Regions of interest (VTA, LEC) were defined based on
539 anatomical landmarks from the Allen Brain Atlas. Co-localization of fluorophores was quantified
540 by calculating overlap of >65% volume between markers (e.g., EYFP/TH or EYFP/VGLUT2).
541 Axon density was computed as the volume of labeled terminals normalized to the total LEC
542 volume. All quantifications were performed by at least two independent investigators blinded to

age group, and quality checks were conducted to ensure reproducibility and consistency across datasets.

**Statistical Analyses.** Statistical analyses were performed using GraphPad Prism, with α set at 0.05. Data distributions were assessed using the Shapiro–Wilk test to determine whether parametric or nonparametric tests were appropriate. Between-group comparisons were analyzed using one-way ANOVA, two-way ANOVA, or repeated-measures ANOVA, followed by Dunnett's or Bonferroni post hoc tests. For non-normally distributed data, Kruskal–Wallis and Mann–Whitney U tests were used with Dunn's post hoc correction when appropriate. Effect sizes are reported as partial eta squared ($\eta p^2$), Cohen's d, or rank-biserial r, depending on the analysis. All statistical tests are reported in the Results and figure legends.

# Resource Availability

N/A

# Lead Contact

Any requests for additional information should be directed to the lead contact, Dr. Susana Mingote (SMinogte@gc.cuny.edu)

# Acknowledgments

This work was supported by the National Institutes of Health (NIH; R21MH123926). **JN** was supported by the NIH, National Institute of General Medical Sciences (NIGMS) Maximizing Access to Research Careers (MARC; 5 T34 GM007639, 5 R25 GM065096). The authors want to acknowledge the Epigenetics Core Facility of CUNY Advanced Science Research Center for instrument use and scientific and technical assistance with the *in situ* hybridization (RNAscope) experiment. Figures were created with BioRender.com.

# Funding

The work was supported by NIH R21MH123926. **JN** was supported by NIH MARC grants 5 T34 GM007639 and 5 R25 GM065096.

# Author contributions

**JNT**: conceptualization, investigation, methodology, data curation, formal analysis, visualization, writing, review and editing. **SF**: investigation, data curation. **AB**: investigation, data curation. **JN**: investigation, data curation. **AL**: data curation, formal analysis, methodology. **YSK**: methodology, resources. **LEF**: methodology, resources, consultation. **CR**: methodology, consultation. **KD**: methodology, resources, consultation. **SM**: conceptualization, funding acquisition, supervision, writing, review, and editing.

# Declaration of Competing Interests

The authors declare no competing interests.

# Supplementary Information

Supplementary information is available for this paper in the form of figures.

# References


Alexander GE, Ryan L, Bowers D, Foster TC, Bizon JL, Geldmacher DS, Glisky EL (2012) Characterizing cognitive aging in humans with links to animal models. Front Ag Neurosci 4 Available at: http://journal.frontiersin.org/article/10.3389/fnagi.2012.00021/abstract [Accessed October 5, 2025].

Bäckman L, Nyberg L, Lindenberger U, Li S-C, Farde L (2006) The correlative triad among aging, dopamine, and cognition: Current status and future prospects. Neuroscience & Biobehavioral Reviews 30:791–807.

Bromberg-Martin ES, Matsumoto M, Hikosaka O (2010) Dopamine in Motivational Control: Rewarding, Aversive, and Alerting. Neuron 68:815–834.

Buck SA, Mabry SJ, Glausier JR, Banks-Tibbs T, Ward C, Kozel J, Fu C, Fish KN, Lewis DA, Logan RW, Freyberg Z (2025) Aging disrupts the coordination between mRNA and protein expression in mouse and human midbrain. Mol Psychiatry Available at: https://www.nature.com/articles/s41380-025-02909-1 [Accessed February 6, 2025].

Buck SA, Torregrossa MM, Logan RW, Freyberg Z (2021) Roles of dopamine and glutamate co-release in the nucleus accumbens in mediating the actions of drugs of abuse. The FEBS Journal 288:1462–1474.

Bunzeck N, Schütze H, Stallforth S, Kaufmann J, Düzel S, Heinze H-J, Düzel E (2007) Mesolimbic Novelty Processing in Older Adults. Cerebral Cortex 17:2940–2948.

Burke SN, Wallace JL, Nematollahi S, Uprety AR, Barnes CA (2010) Pattern separation deficits may contribute to age-associated recognition impairments. Behavioral Neuroscience 124:559–573.

Canto CB, Wouterlood FG, Witter MP (2008) What Does the Anatomical Organization of the Entorhinal Cortex Tell Us? Neural Plasticity 2008:1–18.

Chowdhury R, Guitart-Masip M, Bunzeck N, Dolan RJ, Duzel E (2012) Dopamine Modulates Episodic Memory Persistence in Old Age. Journal of Neuroscience 32:14193–14204.

Conrad WS, Oriol L, Kollman GJ, Faget L, Hnasko TS (2024) Proportion and distribution of neurotransmitter-defined cell types in the ventral tegmental area and substantia nigra pars compacta. Addiction Neuroscience 13:100183.

Deshmukh SS, Knierim JJ (2011) Representation of Non-Spatial and Spatial Information in the Lateral Entorhinal Cortex. Front Behav Neurosci 5 Available at: http://journal.frontiersin.org/article/10.3389/fnbeh.2011.00069/abstract [Accessed August 9, 2020].

Di Lorenzo Alho AT, Suemoto CK, Polichiso L, Tampellini E, De Oliveira KC, Molina M, Santos GAB, Nascimento C, Leite REP, De Lucena Ferreti-Rebustini RE, Da Silva AV, Nitrini R, Pasqualucci CA, Jacob-Filho W, Heinsen H, Grinberg LT (2016) Three-dimensional and stereological characterization of the human substantia nigra during aging. Brain Struct Funct 221:3393–3403.

626 Eskenazi D, Malave L, Mingote S, Yetnikoff L, Ztaou S, Velicu V, Rayport S, Chuhma N (2021)
627 Dopamine Neurons That Cotransmit Glutamate, From Synapses to Circuits to Behavior.
628 Front Neural Circuits 15:665386.

629 Fallon JH, Koziell DA, Moore RY (1978) Catecholamine innervation of the basal forebrain II.
630 Amygdala, suprarhinal cortex and entorhinal cortex. J Comp Neurol 180:509–531.

631 Farassat N, Costa KM, Stojanovic S, Albert S, Kovacheva L, Shin J, Egger R, Somayaji M,
632 Duvarci S, Schneider G, Roeper J (2019) In vivo functional diversity of midbrain
633 dopamine neurons within identified axonal projections. eLife 8:e48408.

634 Fenno LE, Ramakrishnan C, Kim YS, Evans KE, Lo M, Vesuna S, Inoue M, Cheung KYM, Yuen
635 E, Pichamoorthy N, Hong ASO, Deisseroth K (2020) Comprehensive Dual- and Triple-
636 Feature Intersectional Single-Vector Delivery of Diverse Functional Payloads to Cells of
637 Behaving Mammals. Neuron:S0896627320304323.

638 Fleury S, Kolaric R, Espera J, Ha Q, Tomaio J, Gether U, Sørensen AT, Mingote S (2024) Role
639 of dopamine neurons in familiarity. Eur J of Neuroscience:ejn.16326.

640 Gallagher M, Rapp PR (1997) THE USE OF ANIMAL MODELS TO STUDY THE EFFECTS OF
641 AGING ON COGNITION. Annu Rev Psychol 48:339–370.

642 Hernández-Frausto M, Vivar C (2024) Entorhinal cortex–hippocampal circuit connectivity in
643 health and disease. Front Hum Neurosci 18:1448791.

644 Hirsch E, Graybiel AM, Agid YA (1988) Melanized DAergic neurons are differentially susceptible
645 to degeneration in Parkinson's disease. Nature 334:345–348.

646 Huang Y-Y, Kandel ER (1995) D1/D5 receptor agonists induce a protein synthesis-dependent
647 late potentiation in the CAl region of the hippocampus. Proceedings of the National
648 Academy of Sciences 92:2446–2450.

649 Hunsaker MR, Chen V, Tran GT, Kesner RP (2013) The medial and lateral entorhinal cortex
650 both contribute to contextual and item recognition memory: A test of the binding ofitems
651 and context model. Hippocampus 23:380–391.

652 Ito HT, Schuman EM (2012) Functional division of hippocampal area CA1 via modulatory gating
653 of entorhinal cortical inputs. Hippocampus 22:372–387.

654 Johansson J, Nordin K, Pedersen R, Karalija N, Papenberg G, Andersson M, Korkki SM,
655 Riklund K, Guitart-Masip M, Rieckmann A, Bäckman L, Nyberg L, Salami A (2023)
656 Biphasic patterns of age-related differences in dopamine D1 receptors across the adult
657 lifespan. Cell Reports 42:113107.

658 Karalija N, Johansson J, Papenberg G, Wåhlin A, Salami A, Köhncke Y, Brandmaier AM,
659 Andersson M, Axelsson J, Riklund K, Lövdén M, Lindenberger U, Bäckman L, Nyberg L
660 (2022) Longitudinal Dopamine D2 Receptor Changes and Cerebrovascular Health in
661 Aging. Neurology 99 Available at:
662 https://www.neurology.org/doi/10.1212/WNL.0000000000200891 [Accessed March 29,
663 2024].

664 Kempadoo KA, Mosharov EV, Choi SJ, Sulzer D, Kandel ER (2016) Dopamine release from the
665 locus coeruleus to the dorsal hippocampus promotes spatial learning and memory. Proc
666 Natl Acad Sci USA 113:14835–14840.

667 Khan UA, Liu L, Provenzano FA, Berman DE, Profaci CP, Sloan R, Mayeux R, Duff KE, Small
668 SA (2014) Molecular drivers and cortical spread of lateral entorhinal cortex dysfunction
669 in preclinical Alzheimer's disease. Nat Neurosci 17:304–311.

670 Kutlu MG, Zachry JE, Melugin PR, Cajigas SA, Chevee MF, Kelly SJ, Kutlu B, Tian L, Siciliano
671 CA, Calipari ES (2021) Dopamine release in the nucleus accumbens core signals
672 perceived saliency. Current Biology 31:4748-4761.e8.

673 Leal SL, Yassa MA (2015) Neurocognitive Aging and the Hippocampus across Species. Trends
674 in Neurosciences 38:800–812.

675 Lee JY, Jun H, Soma S, Nakazono T, Shiraiwa K, Dasgupta A, Nakagawa T, Xie JL, Chavez J,
676 Romo R, Yungblut S, Hagihara M, Murata K, Igarashi KM (2021) Dopamine facilitates
677 associative memory encoding in the entorhinal cortex. Nature Available at:
678 https://www.nature.com/articles/s41586-021-03948-8 [Accessed September 30, 2021].

679 Li S, Cullen WK, Anwyl R, Rowan MJ (2003) Dopamine-dependent facilitation of LTP induction
680 in hippocampal CA1 by exposure to spatial novelty. Nat Neurosci 6:526–531.

681 Lisman JE, Otmakhova NA (2001) Storage, recall, and novelty detection of sequences by the
682 hippocampus: Elaborating on the SOCRATIC model to account for normal and aberrant
683 effects of dopamine. Hippocampus 11:551–568.

684 Ma, Röytt, Collan, Rinne (1999) Unbiased morphometrical measurements show loss of
685 pigmented nigral neurones with ageing. Neuropathology Appl Neurobio 25:394–399.

686 McGovern DJ, Phillips A, Ly A, Prévost ED, Ward L, Siletti K, Kim YS, Fenno LE, Ramakrishnan
687 C, Deisseroth K, Ford CP, Root DH (2024) Salience signaling and stimulus scaling of
688 ventral tegmental area glutamate neuron subtypes. Available at:
689 http://biorxiv.org/lookup/doi/10.1101/2024.06.12.598688 [Accessed June 24, 2024].

690 Meng D, Li H, Deisseroth K, Leutgeb S, Spitzer NC (2018) Neuronal activity regulates
691 neurotransmitter switching in the adult brain following light-induced stress. Proc Natl
692 Acad Sci USA 115:5064–5071.

693 Mingote S, Amsellem A, Kempf A, Rayport S, Chuhma N (2019) Dopamine-glutamate neuron
694 projections to the nucleus accumbens medial shell and behavioral switching.
695 Neurochemistry International 129:104482.

696 Mingote S, Chuhma N, Kalmbach A, Thomsen GM, Wang Y, Mihali A, Sferrazza C, Zucker-
697 Scharff I, Siena A-C, Welch MG, Lizardi-Ortiz J, Sulzer D, Moore H, Gaisler-Salomon I,
698 Rayport S (2017) Dopamine neuron dependent behaviors mediated by glutamate
699 cotransmission. eLife 6:e27566.

700 Mingote S, Chuhma N, Kusnoor SV, Field B, Deutch AY, Rayport S (2015) Functional
701 Connectome Analysis of Dopamine Neuron Glutamatergic Connections in Forebrain
702 Regions. J Neurosci 35:16259–16271.

703 Morcom AM, Bullmore ET, Huppert FA, Lennox B, Praseedom A, Linnington H, Fletcher PC
704 (2010) Memory Encoding and Dopamine in the Aging Brain: A Psychopharmacological
705 Neuroimaging Study. Cerebral Cortex 20:743–757.

706 Nakagawa T, Xie JL, Savadkohighodjanaki M, Zhang YJ, Jun H, Cao K, Ichii A, Lee JY, Soma
707 S, Medhat YK, Saido TC, Igarashi KM (2024) Early disruption of entorhinal dopamine in
708 a knock-in model of Alzheimer's disease. Available at:
709 http://biorxiv.org/lookup/doi/10.1101/2024.10.10.617678 [Accessed October 5, 2025].

710 Nobili A et al. (2017) Dopamine neuronal loss contributes to memory and reward dysfunction in
711 a model of Alzheimer's disease. Nat Commun 8:14727.

712 Nordin K, Gorbach T, Pedersen R, Panes Lundmark V, Johansson J, Andersson M, McNulty C,
713 Riklund K, Wåhlin A, Papenberg G, Kalpouzos G, Bäckman L, Salami A (2022)
714 DyNAMiC : A prospective longitudinal study of dopamine and brain connectomes: A new
715 window into cognitive aging. J of Neuroscience Research 100:1296–1320.

716 Norman KA, Schacter DL (1997) False recognition in younger and older adults: Exploring the
717 characteristics of illusory memories. Memory & Cognition 25:838–848.

718 Osorio-Gómez D, Guzmán-Ramos K, Bermúdez-Rattoni F (2022) Dopamine activity on the
719 perceptual salience for recognition memory. Front Behav Neurosci 16:963739.

720 Persson BM, Ambrozova V, Duncan S, Wood ER, O'Connor AR, Ainge JA (2022) Lateral
721 entorhinal cortex lesions impair odor-context associative memory in male rats. J of
722 Neuroscience Research 100:1030–1046.

723 Poulin J-F, Caronia G, Hofer C, Cui Q, Helm B, Ramakrishnan C, Chan CS, Dombeck DA,
724 Deisseroth K, Awatramani R (2018) Mapping projections of molecularly defined
725 dopamine neuron subtypes using intersectional genetic approaches. Nat Neurosci
726 21:1260–1271.

727 Rapp PR, Gallagher M (1996) Preserved neuron number in the hippocampus of aged rats with
728 spatial learning deficits. Proc Natl Acad Sci USA 93:9926–9930.

729 Reagh Z, Yassa M (2017) Selective vulnerabilities and biomarkers in neurocognitive aging.
730 F1000Res 6:491.

731 Reagh ZM, Ho HD, Leal SL, Noche JA, Chun A, Murray EA, Yassa MA (2016) Greater loss of
732 object than spatial mnemonic discrimination in aged adults: SELECTIVE OBJECT
733 MEMORY DEFICITS IN AGING. Hippocampus 26:417–422.

734 Reagh ZM, Noche JA, Tustison NJ, Delisle D, Murray EA, Yassa MA (2018) Functional
735 Imbalance of Anterolateral Entorhinal Cortex and Hippocampal Dentate/CA3 Underlies
736 Age-Related Object Pattern Separation Deficits. Neuron 97:1187-1198.e4.

737 Root DH, Wang H-L, Liu B, Barker DJ, Mód L, Szocsics P, Silva AC, Maglóczky Z, Morales M
738 (2016) Glutamate neurons are intermixed with midbrain dopamine neurons in nonhuman
739 primates and humans. Sci Rep 6:30615.

740 Schnell SA, Staines WA, Wessendorf MW (1999) Reduction of Lipofuscin-like Autofluorescence
741 in Fluorescently Labeled Tissue. J Histochem Cytochem 47:719–730.

742 Schultz W (1998) Predictive Reward Signal of Dopamine Neurons. Journal of Neurophysiology
743 80:1–27.

744 Serra L, D'Amelio M, Di Domenico C, Dipasquale O, Marra C, Mercuri NB, Caltagirone C,
745 Cercignani M, Bozzali M (2018) In vivo mapping of brainstem nuclei functional
746 connectivity disruption in Alzheimer's disease. Neurobiology of Aging 72:72–82.

747 Small SA, Swanson LW (2018) A Network Explanation of Alzheimer's Regional Vulnerability.
748 Cold Spring Harb Symp Quant Biol 83:193–200.

749 Smith CC, Greene RW (2012) CNS Dopamine Transmission Mediated by Noradrenergic
750 Innervation. J Neurosci 32:6072–6080.

751 Stuber GD, Hnasko TS, Britt JP, Edwards RH, Bonci A (2010) DAergic Terminals in the Nucleus
752 Accumbens But Not the Dorsal Striatum Corelease Glutamate. Journal of Neuroscience
753 30:8229–8233.

754 Sulzer D, Cragg SJ, Rice ME (2016) Striatal dopamine neurotransmission: Regulation of
755 release and uptake. Basal Ganglia 6:123–148.

756 Swanson LW (1982) The Projections of the Ventral Tegmental Area and Adjacent Regions: A
757 Combined Fluorescent Retrograde Tracer and Immunofluorescence Study in the Rat.
758 Brain Research Bulletin 9:321–353.

759 Takeuchi T, Duszkiewicz AJ, Sonneborn A, Spooner PA, Yamasaki M, Watanabe M, Smith CC,
760 Fernández G, Deisseroth K, Greene RW, Morris RGM (2016) Locus coeruleus and
761 DAergic consolidation of everyday memory. Nature 537:357–362.

762 Tran T, Bridi M, Koh MT, Gallagher M, Kirkwood A (2019) Reduced cognitive performance in
763 aged rats correlates with increased excitation/inhibition ratio in the dentate gyrus in
764 response to lateral entorhinal input. Neurobiology of Aging 82:120–127.

765 Tran TT, Speck CL, Gallagher M, Bakker A (2022) Lateral entorhinal cortex dysfunction in
766 amnestic mild cognitive impairment. Neurobiology of Aging 112:151–160.

767 Tritsch NX, Ding JB, Sabatini BL (2012) DAergic neurons inhibit striatal output through non-
768 canonical release of GABA. Nature 490:262–266.

769 Tsao A, Moser M-B, Moser EI (2013) Traces of Experience in the Lateral Entorhinal Cortex.
770 Current Biology 23:399–405.

771 Tsetsenis T, Broussard JI, Dani JA (2023) DAergic regulation of hippocampal plasticity,
772 learning, and memory. Front Behav Neurosci 16:1092420.

773 Vandrey B, Garden DLF, Ambrozova V, McClure C, Nolan MF, Ainge JA (2020) Fan Cells in
774 Layer 2 of the Lateral Entorhinal Cortex Are Critical for Episodic-like Memory. Current
775 Biology 30:169-175.e5.

776 Wang C, Lee H, Rao G, Doreswamy Y, Savelli F, Knierim JJ (2023) Superficial-layer versus
777 deep-layer lateral entorhinal cortex: Coding of allocentric space, egocentric space,
778 speed, boundaries, and corners. Hippocampus 33:448–464.

779 Wang DV, Viereckel T, Zell V, Konradsson-Geuken Å, Broker CJ, Talishinsky A, Yoo JH,
780 Galinato MH, Arvidsson E, Kesner AJ, Hnasko TS, Wallén-Mackenzie Å, Ikemoto S
781 (2017) Disrupting Glutamate Co-transmission Does Not Affect Acquisition of Conditioned
782 Behavior Reinforced by Dopamine Neuron Activation. Cell Reports 18:2584–2591.

783 Warlow SM, Singhal SM, Hollon NG, Faget L, Dowlat DS, Zell V, Hunker AC, Zweifel LS,
784 Hnasko TS (2024) Mesoaccumbal glutamate neurons drive reward via glutamate release
785 but aversion via dopamine co-release. Neuron 112:488-499.e5.

786 Wilson IA, Gallagher M, Eichenbaum H, Tanila H (2006) Neurocognitive aging: prior memories
787 hinder new hippocampal encoding. Trends in Neurosciences 29:662–670.

788 Witter MP, Doan TP, Jacobsen B, Nilssen ES, Ohara S (2017) Architecture of the Entorhinal
789 Cortex A Review of Entorhinal Anatomy in Rodents with Some Comparative Notes.
790 Front Syst Neurosci 11:46.

791 Wu X, Hammer JA (2021) ZEISS Airyscan: Optimizing Usage for Fast, Gentle, Super-
792 Resolution Imaging. In: Confocal Microscopy (Brzostowski J, Sohn H, eds), pp 111–130
793 Methods in Molecular Biology. New York, NY: Springer US. Available at:
794 https://link.springer.com/10.1007/978-1-0716-1402-0_5 [Accessed October 5, 2025].

795 Yamaguchi T, Qi J, Wang H, Zhang S, Morales M (2015) Glutamatergic and DAergic neurons in
796 the mouse ventral tegmental area. Eur J of Neuroscience 41:760–772.

797 Yassa MA, Lacy JW, Stark SM, Albert MS, Gallagher M, Stark CEL (2010) Pattern separation
798 deficits associated with increased hippocampal CA3 and dentate gyrus activity in
799 nondemented older adults. Hippocampus:n/a-n/a.